May–September precipitation in the Bhutan Himalaya since 1743 as reconstructed from tree ring cellulose $\delta^{18}O$

Masaki Sano,[1] Phuntsho Tshering,[1,2] Jiro Komori,[1,2] Koji Fujita,[1] Chenxi Xu,[1] and Takeshi Nakatsuka[1]

Received 25 April 2013; revised 17 July 2013; accepted 18 July 2013; published 13 August 2013.

[1] We developed a 50-year tree ring $\delta^{18}O$ chronology for each of three tree species (*Juniperus indica*, *Larix griffithii*, and *Picea spinulosa*) using a total of 12 trees (four trees per species) from the Bhutan Himalaya. Despite originating from different species sampled at two different altitudes, the $\delta^{18}O$ chronologies are highly correlated with one another ($r = 0.76$–0.89). Response analyses reveal that tree ring $\delta^{18}O$ values are controlled mainly by summer precipitation, irrespective of species. Based on these results, a robust 269-year $\delta^{18}O$ chronology was established to reconstruct the amount of May–September precipitation based on data from four larch trees. Our tree ring $\delta^{18}O$ data show significant correlations with those from other regions of the Himalaya and the Tibetan Plateau, indicating that common signals related to monsoon activity are recorded in the data. However, at centennial timescales, our data from Bhutan show normal conditions during the 20th century, whereas records from sites in western Nepal and the southern/eastern Tibetan Plateau show weakening trends in monsoon intensity during the last 100–200 years; the weakening trends may be the result of a reduction in the meridional sea surface temperature gradient in the Indian Ocean during this time. At continental scales, the tree ring records show that areas more from ocean basins are particularly sensitive to reduced monsoon circulation. Correlation analyses suggest that the El Niño–Southern Oscillation (ENSO) plays an important role in modulating summer precipitation. However, the teleconnected relationship disappears during the period 1951–1970, coinciding with a negative phase of the Pacific Decadal Oscillation (PDO), implying interdecadal modulation of the PDO on the influence of the ENSO on precipitation in Bhutan.

Citation: Sano, M., P. Tshering, J. Komori, K. Fujita, C. Xu, and T. Nakatsuka (2013), May–September precipitation in the Bhutan Himalaya since 1743 as reconstructed from tree ring cellulose $\delta^{18}O$, *J. Geophys. Res. Atmos.*, *118*, 8399–8410, doi:10.1002/jgrd.50664.

1. Introduction

[2] The climate in South Asia is governed by the Indian monsoon, which is characterized by distinct rainy and dry seasons. The potential impact of hydroclimate regime shifts under changing global climate poses substantive challenges to human activities in the region, and therefore, accurate predictions of future changes in monsoon activity are a matter of societal concern. Because instrumentally observed climate data in South Asia are temporally and spatially limited, longer records derived from paleoclimatic proxies such as tree rings, ice cores, and speleothems are invaluable to an improved understanding of the dynamics and causes of monsoon variability.

[3] Tree rings are one of the most reliable and useful proxies of past climate, as they provide precisely dated time series with annual time resolutions extending back centuries to millennia. Tree ring widths have been widely used to reconstruct past precipitation and temperatures in western (Indian) Himalayan regions [e.g., *Singh and Yadav*, 2005; *Yadav*, 2011; *Yadav et al.*, 1999, 2004]. However, dendroclimatic reconstructions for the central and eastern Himalaya are rather scant, owing largely to the paucity of long meteorological records and the reduced climate sensitivity of tree ring data associated with relatively abundant rainfall. Therefore, statistically calibrated and verified reconstructions for this region (i.e., in Nepal) have been achieved so far by using a dense network of ring width data across the region [*Cook et al.*, 2003] and by developing several chronologies from a single site based on densitometry [*Sano et al.*, 2005]. In addition, the climatic variables used for these reconstructions [*Cook et al.*, 2003; *Sano et al.*, 2005] include only temperature. Recently, *Cook et al.* [2010] produced a gridded spatial reconstruction of the Palmer Drought Severity Index (PDSI) over Asia, including the Himalaya. However, precipitation patterns in the central and eastern Himalaya have yet to be reconstructed. We therefore attempted to reconstruct precipitation variations in the eastern Himalaya (Bhutan)

Additional supporting information may be found in the online version of this article.

[1]Graduate School of Environmental Studies, Nagoya University, Nagoya, Japan.
[2]Department of Geology and Mines, Royal Government of Bhutan, Thimphu, Bhutan.

Corresponding author: M. Sano, Graduate School of Environmental Studies, Nagoya University, Furo-cho, Chikusa-ku, Nagoya 464-8601, Japan. (sano.masaki@b.mbox.nagoya-u.ac.jp)

2169-897X/13/10.1002/jgrd.50664

on the basis of oxygen isotopic data from tree rings. Although a network of ring width chronologies has previously been developed for the Bhutan Himalaya [*Cook et al*., 2010], this study presents the first data on tree ring $\delta^{18}O$ values from this region.

[4] Oxygen isotope ratios of tree ring cellulose are strongly correlated with amounts of precipitation and relative humidity. The correlations stem from the following mechanisms. First, data obtained at low latitudes show that oxygen isotopic compositions of precipitation are typically correlated with amounts of precipitation [*Araguás-Araguás et al*., 1998; *Dansgaard*, 1964]. Tree cellulose synthesized using rain water is, therefore, expected to retain information on amounts of precipitation, based on the isotopic signatures of the precipitation. Second, the isotopic composition of leaf water is influenced by transpiration through stomata, which leads to preferential loss of lighter isotopes (e.g., ^{16}O) and consequent enrichment in heavier isotopes (e.g., ^{18}O) [e.g., *McCarroll and Loader*, 2004; *Robertson et al*., 2001; *Saurer et al*., 1997]. The extent to which oxygen isotopes in leaf water are enriched through transpiration is controlled by relative humidity [e.g., *Saurer et al*., 1997]. Therefore, collectively, oxygen isotope compositions of tree ring cellulose are mostly influenced by the $\delta^{18}O$ values of precipitation and levels of relative humidity. On the other hand, oxygen isotopic compositions are relatively less influenced by nonclimatic factors, such as forest disturbances, which are often recorded in ring width variations [*Li et al*., 2011; *Sano et al*., 2012a, 2012b; *Xu et al*., 2011]. In addition, these two factors recorded in tree ring $\delta^{18}O$ are closely related to monsoon activity (wet-dry conditions). Our previous research conducted in the Nepal Himalaya clearly indicates that oxygen isotopes are much more sensitive to the amount of summer precipitation than are ring widths [*Sano et al*., 2010]. The tree ring $\delta^{18}O$ data are therefore expected to provide a basis for the reconstruction of past hydroclimatic variations related to monsoon activity in the eastern Himalaya, whereas ring width measurements fail to capture this type of climatic information [*Sano et al*., 2010; *Xu et al*., 2011]. In addition to their use in local climate reconstructions, tree ring $\delta^{18}O$ records can be used to investigate long-term changes in atmospheric circulation patterns, such as in the Indian summer monsoon and the El Niño–Southern Oscillation (ENSO) [e.g., *Liu et al*., 2012; *Sano et al*., 2012b], as changes in moisture sources and transport processes result in different $\delta^{18}O$ signatures of regional precipitation [*Araguás-Araguás et al*., 1998; *Tian et al*., 2007].

[5] Climate modeling studies reveal that the Indian summer monsoon is intensified under global warming scenarios [*May*, 2002; *Meehl and Washington*, 1993]. Sediment records from the Arabian Sea [*Anderson et al*., 2002] also indicate a strengthening of monsoon winds over the past several centuries. In contrast, an increasing number of tree ring $\delta^{18}O$ studies reveal a weakening of monsoon intensity [*Grießinger et al*., 2011; *Sano et al*., 2012a; *Xu et al*., 2012] in the Himalaya and on the Tibetan Plateau during the last 100–200 years. Interestingly, patterns of weakening of the summer monsoon in the Himalaya and on the Tibetan Plateau may be complex, as tree ring $\delta^{18}O$ records from the southeastern Tibetan Plateau do not show any significant trends over the last century [*Liu et al*., 2013; *Shi et al*., 2012]. These results indicate the complex nature of monsoon dynamics and suggest that the spatiotemporal coverage of paleoclimatic information must be improved to better understand long-term changes in atmospheric circulation patterns in monsoon Asia.

[6] In the present study, we first explore the climatic potential of 50-year tree ring $\delta^{18}O$ chronologies derived from three different species (*Juniperus indica*, *Larix griffithii*, and *Picea spinulosa*) from the Bhutan Himalaya, in which virgin forests are well preserved. Based on these results, we developed a well-replicated $\delta^{18}O$ chronology from four larch trees over the past 269 years (1743–2011 Common Era (C.E.)). This chronology is used to reconstruct the amount of precipitation during the May–September season and allows a comparison with other published tree ring $\delta^{18}O$ chronologies from the Himalaya and the Tibetan Plateau, especially those that focus on decadal- to centennial-scale variability. We also investigate the linkage of tree ring $\delta^{18}O$ from the Bhutan Himalaya with the ENSO.

2. Materials and Methods

2.1. Study Sites and Sampled Trees

[7] Sampling for the present study was conducted in September 2011 at two sites in the Lunana region of northern Bhutan (Figure 1). The sites, which are approximately 30 km distant from one other, are at different altitudes and exhibit different floras and ecological environments. The Tanza site, which is located near the alpine tree line at an altitude of 4400 m above sea level (masl), is in an open forest dominated by juniper (*Juniperus indica*) trees 5–10 m in height. Because of the harsh environment, single standing trees are often more than 10 m from one another. On the other hand, the Wache site, which is located at an altitude of 3500 masl, is in a relatively closed forest composed of variously sized larch (*Larix griffithii*) and spruce (*Picea spinulosa*). The mature larch and spruce from which we collected samples are approximately 20 m in height. To precisely crossdate the growth rings from the different trees, we obtained 22 cores from 14 juniper trees from the Tanza site, 29 cores from 15 larch trees from the Wache site, and 34 cores from 15 spruce trees from the Wache site. All cores were taken at breast height (1.3 m above the ground) using either a 5 or 12 mm diameter increment borer. The mean diameters at breast height for the sampled trees were 50 cm for Juniper, 80 cm for larch, and 90 cm for spruce.

2.2. Tree Ring Data

[8] The core samples were crossdated by visually matching ring width variations using the standard methodology outlined by *Stokes and Smiley* [1968]. Since patterns of ring width variation are species dependent, crossdating was performed separately for each species. After the assignment of an absolute calendar year to every growth ring, we measured the widths of all dated growth rings using the Velmex measuring system with an accuracy of 0.01 mm. To check for possible dating errors, individual ring width series were statistically compared against a master chronology derived by averaging all series using the program COFECHA [*Holmes*, 1983]. According to the COFECHA results, the mean correlations between individual ring width series and the master chronology were 0.38 for juniper, 0.63 for larch, and 0.47 for spruce. Although the correlations are somewhat low, especially for juniper, the reliability of our dating is

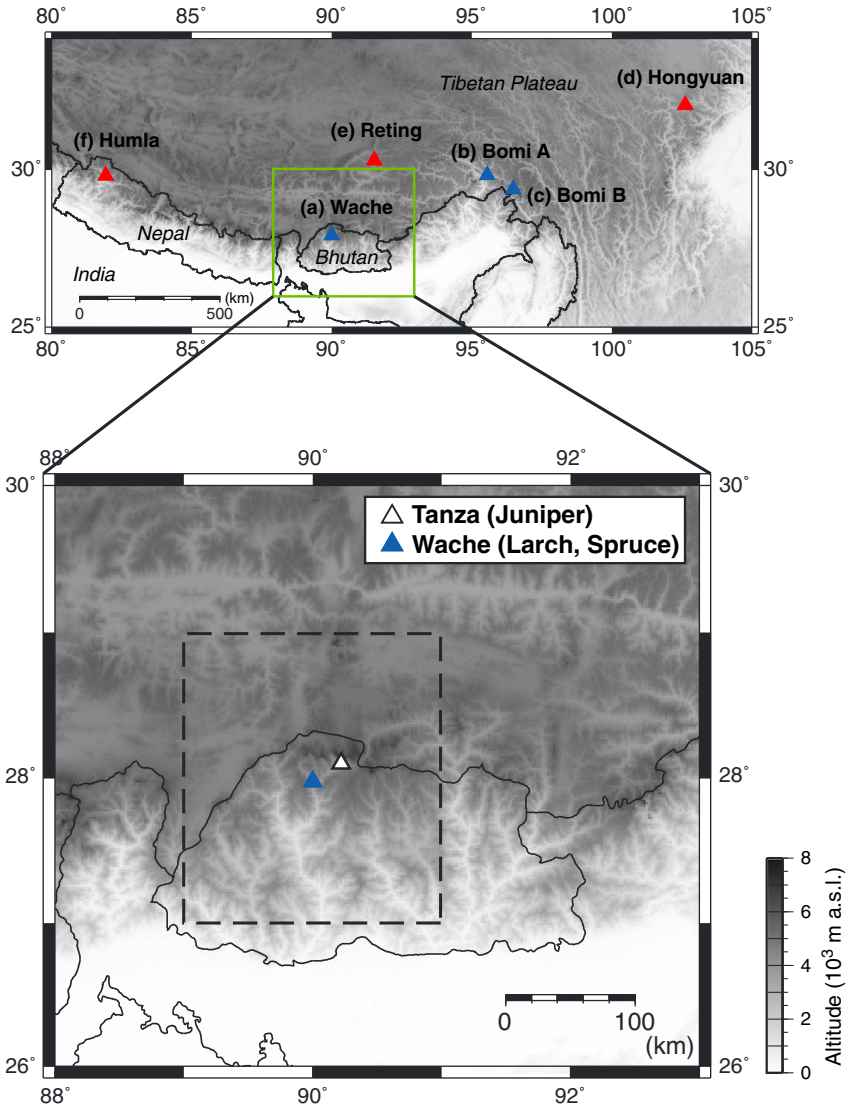

Figure 1. Map of the study region, showing the locations of sites with published tree ring $\delta^{18}O$ chronologies. (top) Published chronologies include (a) the Wache larch chronology from this study, (b) the Bomi A [*Shi et al*., 2012] and (c) Bomi B [*Liu et al*., 2013] sites in the southeastern Tibetan Plateau, (d) the Hongyuan site in the eastern Tibetan Plateau [*Xu et al*., 2012], (e) the Reting site in the southern Tibetan Plateau [*Grießinger et al*., 2011], and (f) the Humla site in western Nepal [*Sano et al*., 2012a]. Sites represented by red (or blue) triangles show weakening trends (or stable states) in monsoon intensity over the last 100–200 years (see text for details), as determined by tree ring $\delta^{18}O$ data. (bottom) Locations of the Tanza (28°06′N, 90°14′E, 4400 masl) and Wache (27°59′N, 90°00′E, 3500 masl) sites of this study. The regional average of the gridded CRU TS3.10 temperature and TS3.10.01 precipitation data sets was derived in the area enclosed by the thick dashed line.

supported by significant correlations of the $\delta^{18}O$ time series data among the different trees (see below).

[9] We selected four cores from four different trees of each species (total of 12 trees) for isotopic analysis. The selection of trees was based on the following two criteria: (1) cores contained as many rings as possible, and (2) growth rings were wide to produce cellulose samples for isotopic analysis. Since the pooling of multiple cores from several trees prior to isotopic analysis constrains the utility of tree ring isotope series, such as evaluating interseries coherence of variation patterns [*McCarroll and Loader*, 2004], isotopic analyses were conducted on each of the 12 cores separately. The analyses were performed on growth rings representing the last 50 years of growth (1962–2011) in each of the 12 cores. In addition, isotopic compositions of all growth rings in the cores of the four larch trees were measured over the entire period of each core (246, 258, 267, and 269 years), and the extended larch record was used to reconstruct the amount of May–September precipitation over the past 269 years (1743–2011 C.E.). We also explored whether age-related biases appear in the larch $\delta^{18}O$ time series by measuring the $\delta^{18}O$ value of the youngest core sample (the shortest duration of 171 years) for the earliest period in which systematically wider rings were produced

(1841–1900). As will be discussed in detail (see below), the age-related effect was not observed in the present study.

[10] The "plate" method was employed to isolate α-cellulose directly from a 1.0 mm thick wood plate of a transverse section, rather than obtaining cellulose from individual rings, so as to facilitate the processing of hundreds of rings simultaneously [*Xu et al*., 2011]. A modified method, which is based on standard protocols [*Green*, 1963; *Loader et al*., 1997], was used to extract cellulose component from whole wood. Each annual ring of cellulose in the plates was separated from adjacent rings using a razor blade under a microscope. The reliability of the plate method was examined for several species, including for larch and spruce, by *Kagawa and Nakatsuka* [2013]. They found no statistically significant difference between tree ring α-cellulose $\delta^{18}O$ values obtained using the plate method and those obtained using conventional methods.

[11] We loaded α-cellulose samples (120–200 μg) into silver foil and determined their $^{18}O/^{16}O$ ratios using a continuous flow isotope ratio mass spectrometer (Thermo Fisher Scientific Delta V Advantage) coupled to an elemental analyzer (Thermo Fisher Scientific Thermal Conversion/Elemental Analyzer) via a Conflo III interface. The $^{18}O/^{16}O$ ratios were expressed as $\delta^{18}O$ (‰), deviations relative to the international Vienna Standard Mean Ocean Water (VSMOW). The analytical uncertainty, derived from a total of 186 measurements of a laboratory standard material (Merck cellulose), was 0.18‰ (1σ). All $\delta^{18}O$ series were individually normalized to have zero mean and unit variance for the common time period of 1962–2011. The resulting series were averaged for each species to construct the final chronology. To examine the strength of common variations among different trees, we computed mean interseries correlation (Rbar) and the expressed population signal (EPS) [*Wigley et al*., 1984], which is calculated using Rbar and the number of samples.

2.3. Climate Analyses

[12] Pearson's correlation coefficients between the $\delta^{18}O$ of tree ring cellulose and monthly climate data within 1-year dendroclimatic windows (October–September) were generated for each species to identify the response of $\delta^{18}O$ values to climate variations. A major difficulty in undertaking dendroclimatic studies in Bhutan is the paucity of long meteorological records that are necessary for climate reconstructions. Most instrumental stations in Bhutan were established after 1984, and the observations often include missing and/or inaccurate data [*Eguchi and Wangda*, 2011]. We therefore utilized the $0.5° \times 0.5°$ gridded Climatic Research Unit (CRU) TS3.10 temperature and TS3.10.01 precipitation data sets (http://badc.nerc.ac.uk/data/cru) [*Harris et al*., 2013], instead of local meteorological data, in this study. The monthly climate values on a 0.5° grid, as derived using triangulated linear interpolation, were based on monthly observations at meteorological stations distributed globally on land areas [*Harris et al*., 2013]. The gridded CRU TS3.10 data (which includes our study region) covers the period 1901–2009. However, we cannot confidently use the data from the first half of the twentieth century, because of the paucity of observations in our study area. We compared monthly precipitation data of the CRU TS3.10.01 data set with those of the "Asian Precipitation–Highly Resolved Observational Data Integration Toward Evaluation of Water Resources (APHRODITE)" [*Yatagai et al*., 2012]; the mean correlation between the two data sets of 0.69 reasonably validates the use of the CRU TS3.10.01 data sets. A regional average of the 16 grid points located in the area from 27.0°N–29.0°N and 89.0°E–91.0°E (see Figure 1) was generated for the response analyses. Correlation coefficients between the tree ring records and the regional climatic data were computed for the common period 1962–2009 (48 years).

[13] An automated weather station installed at 4109 masl in Tanza village, 3 km distant from the Tanza site, provided recent observations on a variety of meteorological parameters during the 3-year period of 2008–2010. The observations were conducted as part of Japan-Bhutan joint research projects that focus mainly on glaciology. Monthly mean temperature, precipitation, and relative humidity during the 3-year period (see Figure S1 in the supporting information) provide a basis for understanding the general climate of the region. The mean annual precipitation was 762.3 mm, 70.9% of which fell in the summer monsoon season of June–September. Premonsoon (March–May) and postmonsoon (October) rainfall contributed 25.8% of the annual precipitation. The mean monthly temperature ranges from 9.3°C (July) to −3.8°C (February). The mean monthly relative humidity ranges from 90.7% (August) to 50.6% (January).

[14] To explore the impacts of El Niño–Southern Oscillation (ENSO) on local climate in Bhutan, our larch chronology was correlated with NINO3.4 sea surface temperatures (SSTs) derived from the HadISST1 data set [*Rayner et al*., 2003] for the period 1901–2011. As the relationship between the ENSO and local climate may not be temporally stable, as indicated by *Liu et al*. [2012] and *Wilson et al*. [2010], correlation analyses were also conducted by separating the entire period into several time spans.

3. Results and Discussion

3.1. Intraspecies and Interspecies Variations in Tree Ring $\delta^{18}O$

[15] Figure 2 shows intraspecies variations in tree ring $\delta^{18}O$ for juniper, larch, and spruce during the past 50 years (1962–2011). The means (and standard deviations) of $\delta^{18}O$ values calculated for individual trees range from 22.33‰ (1.24‰) to 23.08‰ (1.50‰) for juniper, 19.22‰ (1.10‰) to 19.57‰ (1.21‰) for larch, and 21.81‰ (0.99‰) to 24.34‰ (1.08‰) for spruce. The ranges of intertree mean values were 0.75‰ for juniper, 0.35‰ for larch, and 2.53‰ for spruce. Relatively higher intertree differences were observed in the spruce data. However, the variability, which is in the range of 1‰–4‰, is typical of intertree variations observed in previous studies [*Leavitt*, 2010]. Mean intertree correlations (Rbar) were 0.79 for juniper, 0.88 for larch, and 0.74 for spruce. We evaluated the chronology signal strength using the expressed population signal (EPS) [*Wigley et al*., 1984], which indicates how well the chronology estimates a theoretical infinite population. The EPS statistics (0.94 for juniper, 0.97 for larch, and 0.92 for spruce) exceed the threshold value of 0.85 in all three species, indicating that a well-replicated mean chronology can be developed for each species.

[16] To understand interspecies differences in tree ring $\delta^{18}O$ values, we averaged the $\delta^{18}O$ values of the four individual trees in each species (Figure 3). The means (and

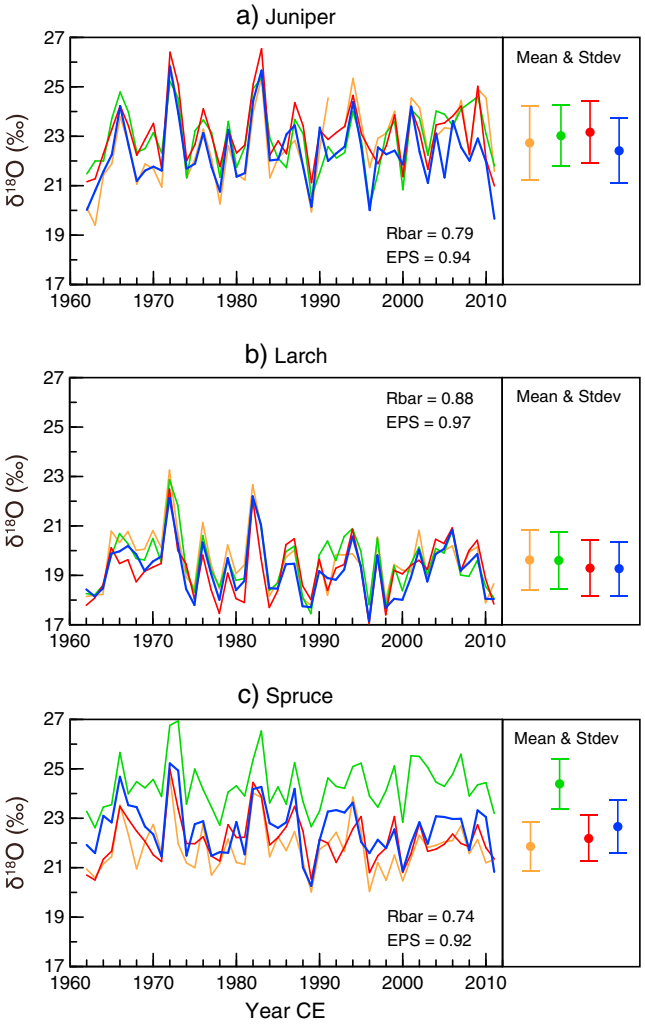

Figure 2. Tree ring $\delta^{18}O$ series for individual (a) juniper, (b) larch, and (c) spruce trees, and the means and standard deviations of the $\delta^{18}O$ values of each tree (right side). Rbar is the mean interseries correlation; EPS is the expressed population signal.

standard deviations) of $\delta^{18}O$ values are 22.75‰ (1.22‰) for juniper, 19.40‰ (1.09‰) for larch, and 22.72‰ (0.90‰) for spruce. The mean for larch is 3.32‰ lower than that for spruce, despite the fact that these trees grow at the same site. *Li et al.* [2011] also reported that the mean $\delta^{18}O$ for larch was 1.5‰ lower than that of spruce, although their sampled trees were located at a site in northern China. We attribute the relatively lower $\delta^{18}O$ value in larch to species-specific physiological differences. It is well known that the oxygen in carbohydrate, which is synthesized in the leaf, undergoes partial exchange with oxygen in xylem water during cellulose synthesis [e.g., *Roden et al.*, 2000]. The fraction of carbohydrate oxygen that undergoes exchange with oxygen of xylem water, and the net fractionation factor between them are likely to be species dependent. It is also possible that differences in root depth and growing season contribute to the $\delta^{18}O$ differences between larch and spruce.

[17] Although absolute $\delta^{18}O$ values vary depending on species, the tree ring $\delta^{18}O$ chronologies of different species are highly correlated with one another ($r = 0.76$–0.89), indicating that common signals related to regional climate are preserved in all three tree species. Interestingly, the correlation coefficients are lower between spruce and larch than they are between spruce and juniper, despite the fact that the spruce and larch chronologies originate from the same sampling site. Overall, the high Rbar and EPS values in larch, as compared with those in spruce and juniper, indicate that from among the trees in this study, the larch chronology is likely the most promising source of time series data for capturing past climate changes.

3.2. Climatic Signals in Tree Ring $\delta^{18}O$

[18] The climatic responses of tree ring $\delta^{18}O$ values are generally consistent among different species, as noted by the highly significant interspecies correlations (Figure 4). However, the tree ring $\delta^{18}O$ chronology derived from juniper shows that juniper $\delta^{18}O$ values are negatively correlated with amounts of precipitation in June and July and positively correlated with July temperature. The larch chronology shows that larch $\delta^{18}O$ values are negatively correlated with amounts of precipitation in June, July, and September and positively correlated with July temperature. The spruce chronology (originating from the same site as that for larch) shows that spruce $\delta^{18}O$ values are negatively correlated with amounts of precipitation in June and July, whereas no significant correlation is observed with temperature. In addition, a composite chronology, calculated as the mean of the three chronologies, shows significant negative correlations with only June and July precipitation (data not shown).

[19] To determine which climatic factor most influences $\delta^{18}O$ values at different times of the year (the amount of precipitation or temperature), each chronology was further correlated with seasonalized precipitation and temperature values. The results show that precipitation is the primary influence on variations in tree ring $\delta^{18}O$ values in all three species (Table 1). However, the seasonal influence of precipitation on $\delta^{18}O$ values is species specific, being June and July for juniper, May–September for larch, and May–July for spruce. Finally, only the juniper chronology shows significant correlations with seasonalized temperatures.

[20] As noted earlier, tree ring $\delta^{18}O$ values are mostly governed by two climatic variables: the $\delta^{18}O$ of source water (precipitation) and relative humidity [e.g., *McCarroll and Loader*, 2004; *Robertson et al.*, 2001; *Saurer et al.*, 1997].

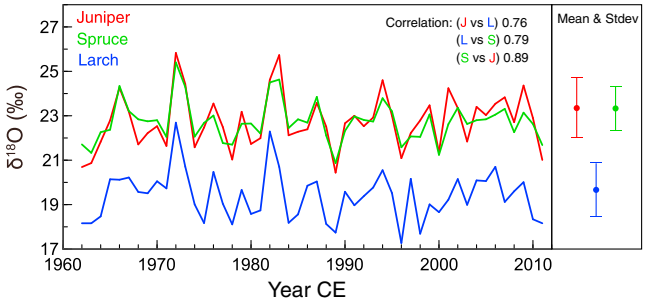

Figure 3. Mean tree ring $\delta^{18}O$ data for juniper (red line), larch (blue line), and spruce (green line), calculated by averaging the $\delta^{18}O$ series of the four trees of each species. The means and standard deviations of the averaged $\delta^{18}O$ values of each species are presented on the right side.

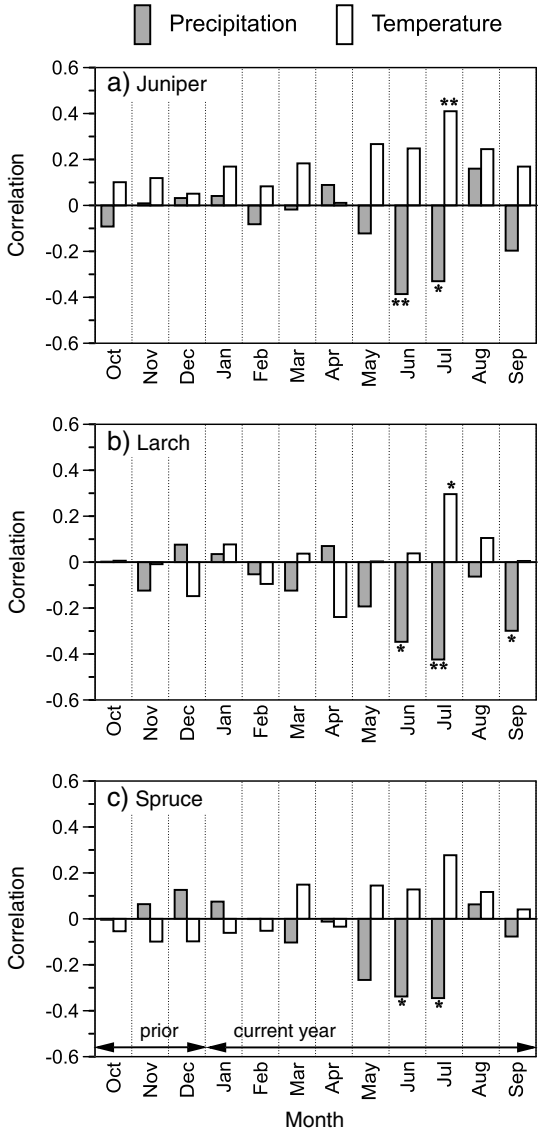

Figure 4. Correlations between tree ring $\delta^{18}O$ and monthly precipitation (shaded bars) and temperature (open bars) for the period 1962–2009, for (a) juniper, (b) larch, and (c) spruce. Averaged monthly precipitation and temperature (October–September) are from the CRU TS3.10.01 and TS3.10 data sets, respectively.

The $\delta^{18}O$ value of precipitation is negatively correlated with the amount of precipitation at low latitudes, which is known as the "amount effect" [*Araguás-Araguás et al*., 1998; *Dansgaard*, 1964]. Specifically, lesser amounts of precipitation correlate with higher $\delta^{18}O$ values of the precipitation, representing a $\delta^{18}O$ enrichment of the source water. Therefore, the negative correlations between tree ring $\delta^{18}O$ and local precipitation can be explained by the amount effect. On the other hand, we were not able to evaluate the effect of humidity on tree ring $\delta^{18}O$ as instrumental records for relative humidity in the area are not available. However, relative humidity levels usually correlate with rainfall, and thus, the two parameters may not be independent of one another. More specifically, lower precipitation levels are usually associated with lower relative humidity. This causes higher gradients of vapor pressure between the atmosphere and leaf interstitial spaces, leading to preferential loss of the lighter isotopes and consequent enrichment in leaf water $\delta^{18}O$ [e.g., *Robertson et al*., 2001; *Roden et al*., 2000].

[21] The positive correlations between juniper tree ring $\delta^{18}O$ and seasonalized temperatures can be explained by the following mechanism. Warmer conditions enhance evaporation of soil water, contributing to $\delta^{18}O$ enrichment of source water that trees take up. It should also be noted that temperature usually shows a negative correlation with the amount of precipitation, indicating that temperature and precipitation may not be independent of one another. In fact, July temperatures showing significant associations with juniper and larch $\delta^{18}O$ values are significantly correlated with July precipitation in the study region ($r = -0.51$, $p < 0.01$). Nevertheless, our overall results can be explained by the theory of oxygen isotopes in tree rings and are consistent with previous findings obtained from the Nepal Himalaya [*Sano et al*., 2010, 2012a] and the Tibetan Plateau [*Grießinger et al*., 2011; *Shi et al*., 2011].

[22] To further confirm the reliability of the precipitation signals identified from the area averages of gridded precipitation records, we conducted a spatial correlation analysis between tree ring $\delta^{18}O$ values and the gridded precipitation data at all grid nodes in the area of 22.0°N–32.0°N and 85.0°E–95.0°E. The highest correlations generally appear in an area that contains the sampling site, indicating that our tree ring $\delta^{18}O$ values for all three species accurately reflect regional precipitation (Figures 5 and S2 in the supporting information). Among the different species, relatively higher correlations occur for the larch data than for the spruce and juniper data. We therefore decided to extend the larch chronology into the preinstrumental era to reconstruct the regional precipitation history over the past 269 years.

3.3. Extended Larch Chronology and Precipitation Reconstruction

[23] Our extended larch $\delta^{18}O$ time series from the four trees are highly correlated with one another for the past 269 years, as seen with high running Rbar statistics (0.85–0.93) computed

Table 1. Correlations Between Tree Ring $\delta^{18}O$ and Seasonalized Precipitation and Temperatures for the Period 1962–2009[a]

	Juniper		Larch		Spruce	
Season	Precipitation	Temperature	Precipitation	Temperature	Precipitation	Temperature
May–July	−0.502**	0.396**	−0.550**	0.121	**−0.521****	0.231
June–July	**−0.507****	0.407**	−0.534**	0.199	−0.479**	0.248
June–September	−0.424**	0.356*	−0.587**	0.144	−0.405**	0.186
May–September	−0.429**	0.383**	**−0.600****	0.113	−0.450**	0.202

[a]Single and double asterisks represent significance at the $p < 0.05$ and $p < 0.01$ levels, respectively. The highest correlation for each species is highlighted in bold.

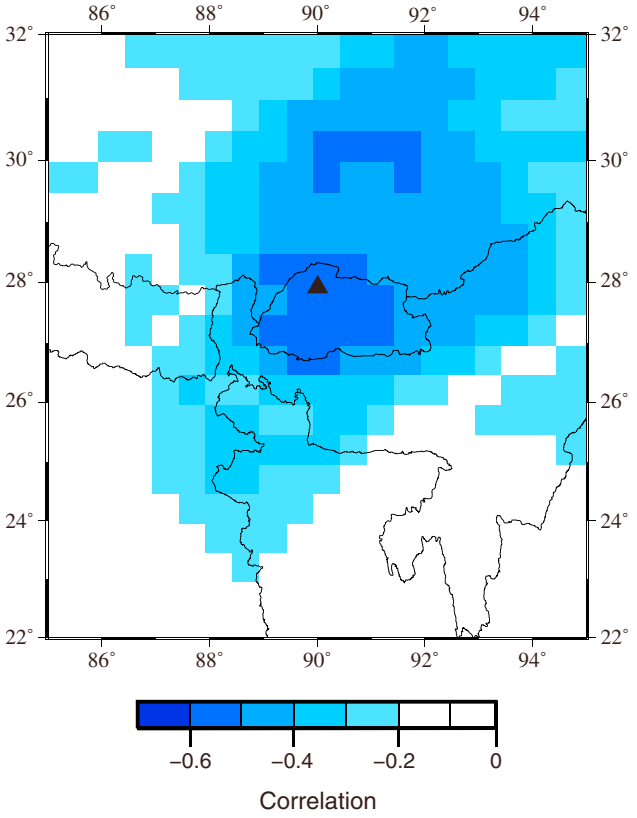

Figure 5. Spatial correlation of larch tree ring $\delta^{18}O$ values with May–September precipitation (CRU TS3.10.01 data set) for the period 1962–2009. Correlations of less than −0.28 are significant at the $p < 0.05$ level. The triangle represents the sampling site.

over 50 years lagged by 25 years (Figure 6). The EPS statistics for the $\delta^{18}O$ data (0.96–0.98) are also sufficiently high to exceed the threshold value of 0.85 for the past 269 years. Our chronology can therefore be considered to provide a reliable estimate of the mean for tree ring $\delta^{18}O$ in the study region.

[24] It has been reported that age-dependent long-term trends often appear in tree ring $\delta^{18}O$ time series data [e.g., *Esper et al*., 2010; *Treydte et al*., 2006]. These studies have identified a decrease in $\delta^{18}O$ values with increasing age, a common trend irrespective of locations and species. We therefore explored whether the age-related effect biases low-frequency variations in the extended larch $\delta^{18}O$ chronology, by measuring $\delta^{18}O$ values of the core with the shortest duration (171 rings) for the earliest period of the core (1841–1900). Regarding ring width variations, the rings in this core sample become systematically wider with a decreasing trend, whereas the rings in the core of the longest duration (269 rings) were relatively narrow and exhibited no significant trends during the common period of 1841–1900 (Figure S3a in the supporting information). We plotted $\delta^{18}O$ time series along with a linear regression of trends for the young and old trees (Figure S3b in the supporting information). In both cases, the $\delta^{18}O$ series do not exhibit any significant long-term trends during the common period of 1841–1900, indicating that there is no apparent age-dependent bias. Although the difference in the mean $\delta^{18}O$ values between short- and long-duration samples was 0.86‰, the $\delta^{18}O$ range is only slightly greater than that of 0.60‰, which is the observed $\delta^{18}O$ range among the four larch trees used to construct the final chronology for the common period. In addition, this variability (range of 0.86‰) is on the low end of the range of approximately 1‰–4‰ and is typical of values of intertree variability as reported in the literature [*Leavitt*, 2010]. Therefore, the difference in the absolute values observed between young and old trees does not seem to originate from the age-related effect. In this study, the pith in all five larch cores (four old and one young tree) was absent; therefore, the cambium ages of the earliest rings are considered to exceed at least a few decades. Recently, *Young et al*. [2011] and *Szymczak et al*. [2012] have reported that age-dependent trends are only observed for the earliest 50 years after germination. Based on our results, together with the finding of *Young et al*. [2011] and *Szymczak et al*. [2012], we conclude that the age-related effect does not appear in our larch $\delta^{18}O$ chronology.

[25] The fidelity of the regression model that is utilized to reconstruct the amount of May–September precipitation was scrutinized by conducting split period calibration-verification tests [*Cook and Kairiukstis*, 1990; *Fritts*, 1976], which are widely used in tree-ring-based climate reconstructions. For this analysis, an extended 60-year period of the climate data (1950–2009) was utilized to increase the degrees of freedom while attempting to eliminate possible uncertainties in the earlier period of 1901–1949 attributed to a paucity of observations. Our results showed that the reduction of error [*Fritts*, 1976] was positive: 0.198 for the 1950–1979 verification period and 0.406 for the 1980–2009 verification period. The coefficient of efficiency [*Cook et al*., 1999] was also positive: 0.183 for the 1950–1979 verification period and 0.394 for the 1980–2009 verification period. Any positive value for these two tests indicates predictive skill of the regression model; therefore, the results support the validity of the reconstruction model. We therefore reconstructed the amount of May–September precipitation back to 1743 C.E., based on a linear regression model that accounts for 30.9% of the actual precipitation variance for the period 1950–2009 (Figure 7). Overall, our reconstructed

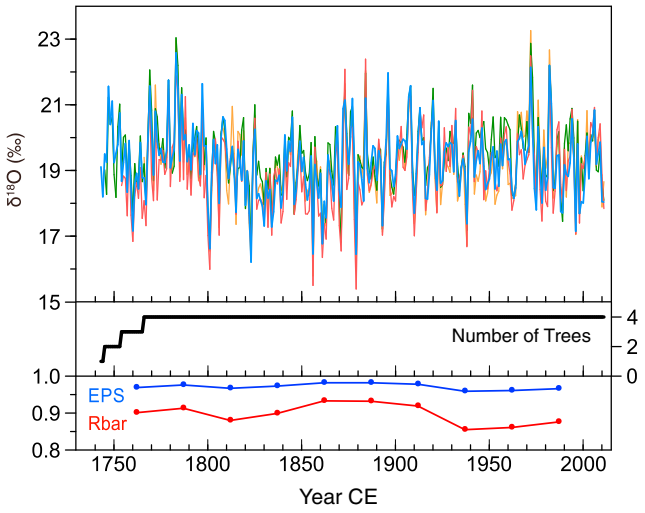

Figure 6. The 269-year larch tree ring $\delta^{18}O$ series (with sample sizes) and running EPS and Rbar values computed over 50 years lagged by 25 years.

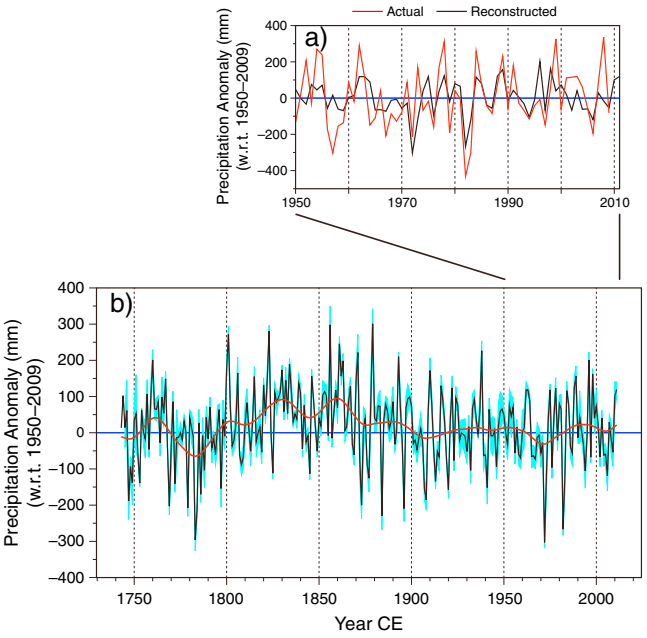

Figure 7. (a) Actual and reconstructed May–September total precipitation for the period 1950–2009. (b) Reconstructed precipitation over the past 269 years (1743–2011 C.E.). The light blue shadows give the 95% confidence limits of the reconstruction. The red line represents 30-year splinted values.

precipitation record reveals that a relatively intense monsoon period in the nineteenth century was followed by a normal period of precipitation in the twentieth century.

3.4. Comparison With Other Proxy Records

[26] We compared our 269-year $\delta^{18}O$ record with previously published tree ring $\delta^{18}O$ chronologies from the Nepal Himalaya [*Sano et al.*, 2012a] and the Tibetan Plateau [*Grießinger et al.*, 2011; *Liu et al.*, 2013; *Shi et al.*, 2012; *Xu et al.*, 2012]. Because the samples in the different studies were collected from different elevations, species, and ecological environments, the climatic parameters and signal seasons vary in the different chronologies. Specifically, the Humla chronology from western Nepal records dry-wet conditions represented by the Palmer Drought Severity Index (PDSI) in the period June–September, while other chronologies from the Tibetan Plateau represent August precipitation [*Grießinger et al.*, 2011], June–August [*Shi et al.*, 2012] and July–August [*Liu et al.*, 2013] cloud cover, and summer precipitation/humidity [*Xu et al.*, 2012]. However, all the chronologies correlate with moisture-related climatic parameters in the summer season, indicating that tree ring $\delta^{18}O$ data in this region is a proxy of monsoon intensity.

[27] As shown in Table 2, our $\delta^{18}O$ chronology shows highly significant correlations ($p < 0.0001$) with those from other regions for the common period 1781–2000, except with the chronology from the eastern Tibetan Plateau [*Xu et al.*, 2012], indicating that common signals related to monsoon activity are recorded in our record. Correlations computed after removing low-frequency variations using 50-year cubic splines [*Cook and Peters*, 1981] are similar to those calculated for the original chronologies. This indicates that high-frequency variations in our tree ring $\delta^{18}O$ data are also shared by those of other chronologies. On the other hand, the correlation matrix given in Table 2 reveals that the Humla chronology from the western Nepal Himalaya [*Sano et al.*, 2012a] and the Hongyuan chronology from the eastern Tibetan Plateau [*Xu et al.*, 2012] are generally less correlated with other chronologies, owing to the different climatic conditions associated with the large geographic separations of the sampling sites.

[28] All the chronologies in Table 2 are plotted in Figure 8, along with smoothed curves emphasizing 50-year variability (note that the normalized $\delta^{18}O$ scales are inverted to fit the precipitation scales; see Figure 1 for locations of study sites). Our chronology is in good agreement with the Bomi "A" chronology [*Shi et al.*, 2012] from the southeastern Tibetan Plateau at multidecadal scales (Figures 8a and 8b). Both chronologies show that an intense monsoon period during the nineteenth century was followed by a normal period in the twentieth century. The Bomi "B" chronology [*Liu et al.*, 2013] also shows an intense monsoon period during the early and midnineteenth century (Figure 8c), but a notable weak monsoon period in the late nineteenth century (unlike the Bomi "A" chronology or our chronology). However, conditions during the twentieth century were normal and without any prominent trends in all three chronologies (Figures 8a, 8b, and 8c), although decadal variations in the Bomi "B" chronology differ somewhat from those of the other two chronologies from the 1980s to the present. Overall, multidecadal variations are generally shared between the Bhutan Himalaya and the southeastern Tibetan Plateau.

[29] In contrast, $\delta^{18}O$ chronologies from the Nepal Himalaya [*Sano et al.*, 2012a] and the southern [*Grießinger et al.*, 2011] and eastern [*Xu et al.*, 2012] Tibetan Plateau reveal a weakening of monsoon precipitation during the past 100–200 years (Figures 8d–8f). Long-term trends of decreasing precipitation are also observed in a varve thickness record from lake sediments [*Chu et al.*, 2011] and a snow accumulation record from an ice core [*Zhao and Moore*,

Table 2. Correlation Matrix Calculated Using the Six Tree Ring $\delta^{18}O$ Chronologies From the Himalaya and Tibet for the Common Period 1781–2000 C.E.[a]

Source Proxy Location	Reference	This Study	*Shi et al.* [2012]	*Liu et al.* [2013]	*Xu et al.* [2012]	*Grießinger et al.* [2011]
SE Tibet (Bomi A)	*Shi et al.* [2012]	0.37 (0.34)				
SE Tibet (Bomi B)	*Liu et al.* [2013]	0.35 (0.35)	0.56 (0.56)			
E Tibet (Hongyuan)	*Xu et al.* [2012]	0.04 ^{ns} (−0.13 ^{ns})	0.03 ^{ns} (−0.12 ^{ns})	0.02 ^{ns} (−0.12 ^{ns})		
S Tibet (Reting)	*Grießinger et al.* [2011]	0.31 (0.31)	0.25 (0.19)	0.36 (0.36)	0.41 (0.03 ^{ns})	
W Nepal (Humla)	*Sano et al.* [2012a]	0.37 (0.40)	0.09 ^{ns} (0.06 ^{ns})	0.17 ^{ns} (0.13 ^{ns})	0.11 ^{ns} (–0.13 ^{ns})	0.37 (0.27)

[a]The values in parentheses were computed after removing low-frequency variations using 50-year cubic splines. The superscript "ns" denotes nonsignificant correlations ($p > 0.01$). See Figure 1 for the locations of the sampling sites.

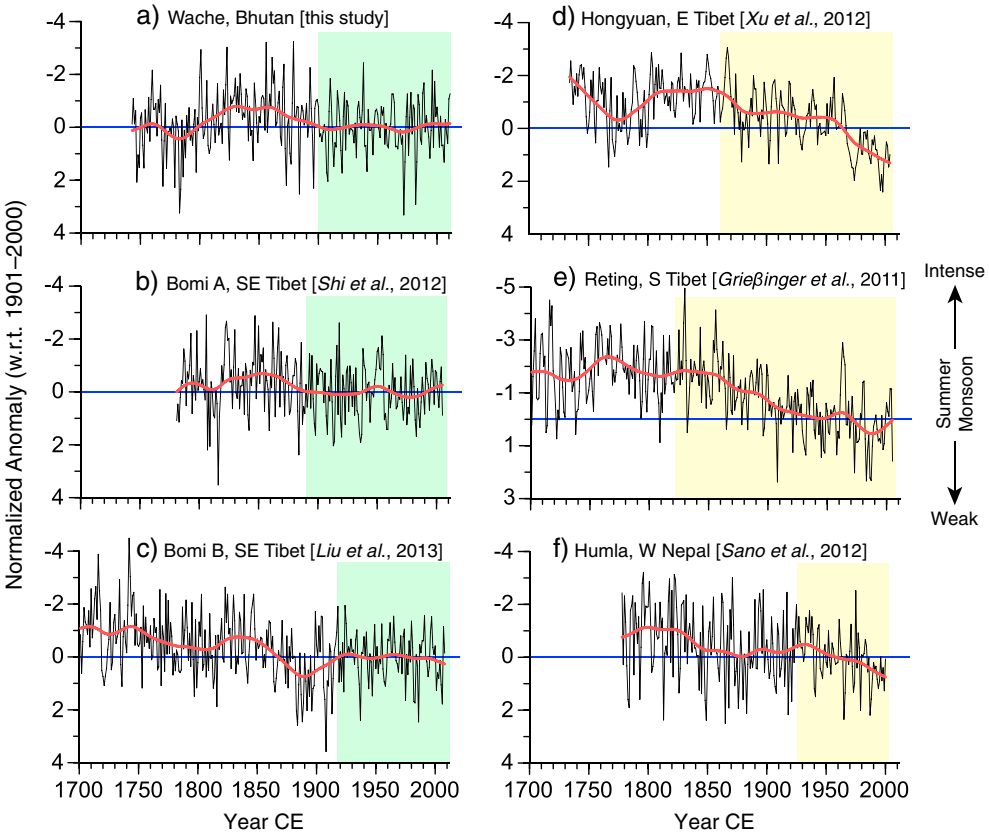

Figure 8. Normalized tree ring $\delta^{18}O$ chronologies from (a) the Wache site in Bhutan (this study), (b) the Bomi A [*Shi et al*., 2012] and (c) the Bomi B sites [*Liu et al*., 2013] in the southeastern Tibetan Plateau, (d) the Hongyuan site in the eastern Tibetan Plateau [*Xu et al*., 2012], (e) the Reting site in the southern Tibetan Plateau [*Grießinger et al*., 2011], and (f) the Humla site in western Nepal [*Sano et al*., 2012a]. The labels Figures 8a–8f correspond to the locations of sites given in Figure 1. All chronologies are normalized to have zero mean and unit variance for the period 1901–2000, and the normalized $\delta^{18}O$ scales are inverted to correspond to the precipitation scales. The 50-year cubic spline curves (red lines) emphasize multidecadal variations. The green (or yellow) shaded areas represent intervals with stable states (or weakening trends) in monsoon intensity. Note that the original records for Figures 8c and 8e cover the past 409 and 842 years, respectively (data prior to 1700 not shown).

2006] from the Tibet Plateau. In addition, analyses based on instrumental data for the last 50 years indicate a weakening of global monsoon rainfall over land [*Wang and Ding*, 2006; *Zhou et al*., 2008b]. Several studies link the reduction in monsoon precipitation with changes in SSTs in the Indian Ocean [e.g., *Chung and Ramanathan*, 2006; *Naidu et al*., 2009; *Zhou et al*., 2008a]. *Chung and Ramanathan* [2006] reported that the 1930–1950 mean SSTs in the Bay of Bengal and northern Arabia Sea were higher than those in the equatorial Indian Ocean in June, thus facilitating the development of the Indian summer monsoon. However, since the 1950s, significant warming has been observed in the equatorial regions of the Indian Ocean, accompanied by minimal warming in its northern regions, leading to a weakening of the meridional SST gradient in the Indian Ocean [*Chung and Ramanathan*, 2006]. Their model simulations reveal that the weakening of the meridional SST gradient lessens monsoon circulation, resulting in reduced monsoon precipitation over India [*Chung and Ramanathan*, 2006]. *Xu et al*. [2012] also associated a weakening of monsoon intensity, as observed in their tree ring $\delta^{18}O$ record from the eastern Tibetan Plateau, with the decreased meridional SST gradient. The detection of a warming trend in a coral-based reconstruction of SSTs for the whole of the tropics (30°N–30°S) [*Wilson et al*., 2006] suggests that SST forcing is likely to explain decreasing trends in monsoon intensity over the last 100–200 years.

[30] Perhaps the most striking difference among the different tree ring $\delta^{18}O$ records is the twentieth century weakening of monsoon intensity observed in the Nepal Himalaya and the southern/eastern Tibetan Plateau (Figures 8d–8f), as compared with the absence of such a trend in the Bhutan Himalaya and the southeastern Tibetan Plateau (Figures 8a–8c). Monsoon depressions normally form in the northern Bay of Bengal and move northwestward along the axis of the monsoon trough, yielding widespread rains [*Pant and Rupa Kumar*, 1997]. Also, water vapor originating in the Bay of Bengal moves northward along the eastern edge of the Tibetan Plateau and enters into China [*Xu et al*., 2012]. The depressions generally weaken with increasing distance of travel from the ocean as the systems become cut off from the moisture supply [*Pant and Rupa Kumar*, 1997]. As shown in Figure 1, the chronologies that show the weakening in monsoon intensity (red triangles) are located relatively

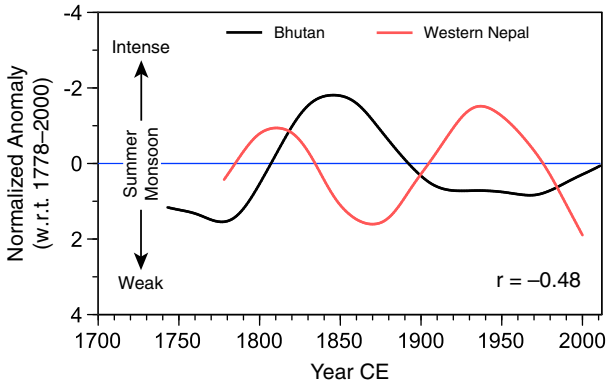

Figure 9. Low-frequency variations in normalized tree ring $\delta^{18}O$ chronologies from Bhutan and western Nepal [*Sano et al.*, 2012a]. Both chronologies are filtered using 100-year cubic splines after detrending linear trends in the chronologies. The normalized $\delta^{18}O$ scales are inverted to correspond to the precipitation scales.

further away from the Bay of Bengal than are those from Bhutan and the southeastern Tibetan Plateau where the weakening is absent (blue triangles). Thus, inland areas appear to be particularly sensitive to the weakening of monsoon circulation.

[31] Interestingly, the phases of low-frequency variations in the tree ring $\delta^{18}O$ chronology from western Nepal are generally opposite those of the Bhutan Himalaya (Figure 9). Note that both chronologies were detrended using linear regression and were filtered to emphasize 100-year variability using cubic splines [*Cook and Peters*, 1981]. At these timescales, variations in the chronologies show a negative correlation of −0.48, while the original records show a positive correlation of 0.37. It is widely recognized that the Indian summer monsoon exhibits intraseasonal oscillations, referred to as "active" and "break" spells, which exhibit quasiperiodic variations of 10–20 days and 30–50 days [e.g., *Krishnamurthy and Shukla*, 2000; *Pant and Rupa Kumar*, 1997; *Webster et al.*, 1998; *Yasunari*, 1979, 1980]. During the "break" spells, the monsoon trough moves northward to the foothills of the Himalaya, resulting in a decrease in rainfall in the central parts of India but enhanced rainfall in the Himalayan foothills of northern India [*Pant and Rupa Kumar*, 1997]. This pattern is reversed during the "active" spells. Empirical orthogonal function (EOF) analysis of summer monsoon precipitation data for the period 1872–1990 at 306 stations distributed across India reveals that the first EOF exhibits a dipole-type spatial structure in precipitation variability [*Pant and Rupa Kumar*, 1997]. Specifically, the northeastern parts of India (and the south of Bhutan) are in one phase while the remainder of the country is in the opposite phase. Therefore, a centennial-scale alternating modality of the intraseasonal oscillations (in which active or break dominates) is possibly responsible for the contrasting phase variations in the tree ring records of western Nepal and Bhutan.

3.5. ENSO Teleconnections With Precipitation in Bhutan

[32] The larch $\delta^{18}O$ chronology exhibits a significant positive correlation ($r = 0.50$, $p < 0.0001$) with May–September NINO3.4 SSTs for the period 1901–2011. This result indicates that El Niño (La Niña) events are generally linked to dry (wet) conditions in the Bhutan Himalaya. In fact, the two most severe droughts in Bhutan in the twentieth century (identified by peak $\delta^{18}O$ values) in 1972 and 1982 corresponded to major El Niño events. The ENSO-monsoon linkage has also been identified in a tree ring $\delta^{18}O$ chronology from northern Vietnam [*Sano et al.*, 2012b]. A striking feature in the record is a significant time-stable correlation with ENSO records for the period 1871–2004, indicating that the hydroclimate of northern Vietnam has been firmly linked to the ENSO at least since the late nineteenth century [*Sano et al.*, 2012b].

[33] The influence of the ENSO on the amount of summer precipitation is known to vary temporally and spatially. *Krishna Kumar et al.* [1999] revealed that the inverse relationship between the ENSO and Indian summer monsoon rainfall, which was present during the 1850s to the 1980s, has since broken down. However, the relationship between the ENSO and our tree ring $\delta^{18}O$ record from Bhutan has remained stable during the period 1971–2011 ($r = 0.61$, $p < 0.0001$) (Figure 10a). In addition, our chronology shows a significant correlation with the ENSO for the period 1901–1950 ($r = 0.49$, $p < 0.001$), but no correspondence during 1951–1970 ($r = 0.10$, $p = 0.69$). These results indicate that the temporal influence of the ENSO on the amount of summer rainfall often differs between Bhutan and India.

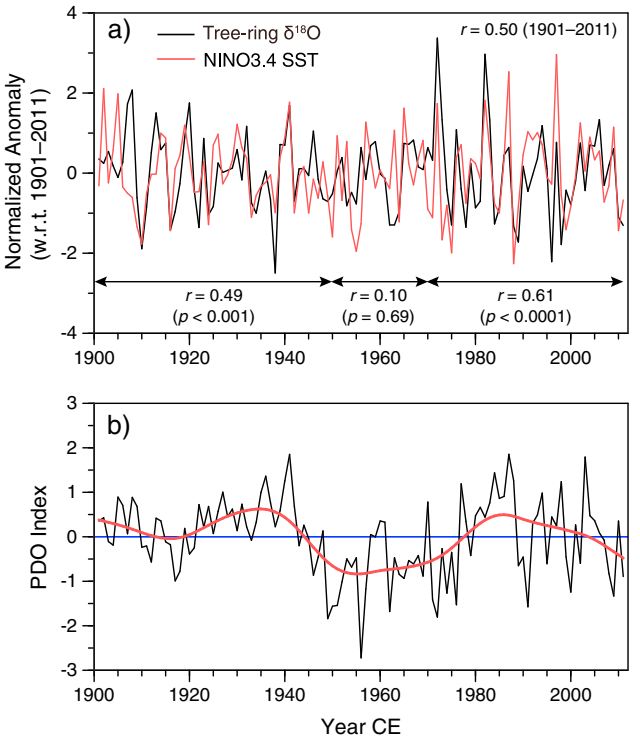

Figure 10. (a) Comparison of the tree ring $\delta^{18}O$ record from the Bhutan Himalaya and May–September NINO 3.4 SSTs, showing correlations between the records for different time periods. (b) Winter (November–March) mean time series of the Pacific Decadal Oscillation (PDO) Index, along with 30-year splined values (red curve) [from *Mantua et al.*, 1997].

Liu et al. [2012] also identified a broken relationship between the ENSO and tree ring $\delta^{18}O$ values from southwestern China during the period 1930–1980, although they were significantly correlated with each other during the periods 1902–1930 and 1980–2004. Interestingly, the temporal patterns of the linkage with ENSO in the southwestern China study area are generally consistent with our results. Specifically, in both records, a broken linkage with the ENSO is found during the midtwentieth century; however, the two records are not exactly matched temporally.

[34] The period 1951–1970, during which the ENSO-rainfall linkage broke down, coincides with a negative phase of the Pacific Decadal Oscillation (PDO) during the period of 1947–1977 [*Mantua et al*., 1997]; moreover, the influence of the ENSO on local rainfall in Bhutan is consistent only during positive phases of the PDO (Figure 10b). *Krishnan and Sugi* [2003] reported that the PDO could play an important role in modulating interannual monsoon variability. Specifically, Indian summer monsoon rainfall more often tends to be below (above) normal when El Niño (La Niña) events occur during positive (negative) phases of the PDO [*Krishnan and Sugi*, 2003]. A similar tendency is also found for the amount of early summer precipitation over South China [*Chan and Zhou*, 2005]. *Krishnan and Sugi* [2003] explained that reinforced SST anomalies resulting from phase-locking of the PDO and the ENSO can alter convective and dynamical fields, producing persistent anomalies over the tropics and the monsoon region. However, our record from Bhutan does not show the tendency observed in India and South China but shows secular variations in the ENSO-rainfall linkage during the negative phase of the PDO (Figure 10b). *Power et al*. [1999] also reported PDO-related secular variations. They found that the relationship between the ENSO and rainfall in Australia is not robust during positive phases of the PDO; moreover, the relationship is consistent only during negative phases of the PDO [*Power et al*., 1999]. Our results, together with the findings of *Power et al*. [1999], imply that the PDO contributes to secular variations in the ENSO-monsoon linkage, although the physical mechanisms underlying the possible contribution have yet to be fully explored.

4. Conclusions

[35] Using $\delta^{18}O$ data from four larch trees, we constructed a well-replicated 269-year $\delta^{18}O$ chronology (1743–2011 C.E.) to reconstruct long-term variations in the amount of May–September precipitation. Our $\delta^{18}O$ data show significant positive correlations with chronologies from other regions of the Himalaya and the Tibetan Plateau for the common period 1781–2000, indicating that common signals are recorded in the chronologies. On the other hand, at centennial timescales, a weakening in monsoon intensity has been observed in the Nepal Himalaya and the southern/eastern Tibetan Plateau, whereas no such trend has been detected in the Bhutan Himalaya or the southeastern Tibetan Plateau. Judging from the locations of tree ring records in this region, inland areas likely receive less intense summer precipitation during periods of weakened monsoon, as opposed to sites closer to the Bay of Bengal, which are not similarly affected. We also found that tree ring $\delta^{18}O$ (and thus the amount of May–September precipitation) in the Bhutan Himalaya is closely linked to the ENSO. However, the link was not observed during 1951–1970, which coincided with a negative phase of the PDO (1947–1977), implying interdecadal modulation of the PDO on the influence of the ENSO on local precipitation in Bhutan. Future research based on an expanded network of tree ring $\delta^{18}O$ chronologies over the Himalaya and the Tibetan Plateau will improve our understanding of the dynamics and causes of monsoon variability in South Asia.

[36] **Acknowledgments.** We are deeply indebted to the Department of Geology and Mines, the Renewable Natural Resources Research Center, and the National Biodiversity Center, Bhutan, for granting us permission to conduct this research. We thank S. Takenaka, K. Ghallay, T. Nuimura, and S. Tsutaki for generous support during fieldwork. We also thank John Bershaw, Matthew Therrell, and an anonymous reviewer for valuable comments and suggestions that improved the manuscript. This study was funded by Grants-in-Aid for Scientific Research from the Japan Society for the Promotion of Science (19253001, 2310262, and 23242047), and a research grant from the Research Institute of Humanity and Nature, Japan.

References

Anderson, D. M., J. T. Overpeck, and A. K. Gupta (2002), Increase in the Asian southwest monsoon during the past four centuries, *Science*, *297*, 596–599.

Araguás-Araguás, L., K. Froehlich, and K. Rozanski (1998), Stable isotope composition of precipitation over southeast Asia, *J. Geophys. Res.*, *103*, 28,721–28,742.

Chan, J. C. L., and W. Zhou (2005), PDO, ENSO and the early summer monsoon rainfall over south China, *Geophys. Res. Lett.*, *32*, L08810, doi:10.1029/2004GL022015.

Chu, G., et al. (2011), Evidence for decreasing South Asian summer monsoon in the past 160 years from varved sediment in Lake Xinluhai, Tibetan Plateau, *J. Geophys. Res.*, *116*, D02116, doi:10.1029/2010JD014454.

Chung, C. E., and V. Ramanathan (2006), Weakening of North Indian SST gradients and the monsoon rainfall in India and the Sahel, *J. Clim.*, *19*, 2,036–2,045.

Cook, E. R., and L. A. Kairiukstis (1990), *Methods of Dendrochronology*, Kluwer, Dordrecht.

Cook, E. R., and K. Peters (1981), The smoothing spline: A new approach to standardizing forest interior tree-ring width series for dendroclimatic studies, *Tree-Ring Bull.*, *41*, 45–53.

Cook, E. R., D. M. Meko, D. W. Stahle, and M. K. Cleaveland (1999), Drought reconstructions for the continental United States, *J. Clim.*, *12*, 1,145–1,163.

Cook, E. R., P. J. Krusic, and P. D. Jones (2003), Dendroclimatic signals in long tree-ring chronologies from the Himalayas of Nepal, *Int. J. Climatol.*, *23*, 707–732.

Cook, E. R., K. J. Anchukaitis, B. M. Buckley, R. D. D'Arrigo, G. C. Jacoby, and W. E. Wright (2010), Asian monsoon failure and megadrought during the last millennium, *Science*, *328*, 486–489.

Dansgaard, W. (1964), Stable isotopes in precipitation, *Tellus*, *16*, 436–468.

Eguchi, T., and P. Wangda (2011), Synoptic and local analysis of relationship between climate and forest in the Bhutan Himalaya (preliminary report), *Working Document 2011/01*, Renewable Natural Resources - Research and Development Centre Yusipang, Dep. of Forests and Park Services, Thimphu.

Esper, J., D. C. Frank, G. Battipaglia, U. Büntgen, C. Holert, K. Treydte, R. Siegwolf, and M. Saurer (2010), Low-frequency noise in $\delta^{13}C$ and $\delta^{18}O$ tree ring data: A case study of *Pinus uncinata* in the Spanish Pyrenees, *Global Biogeochem. Cycles*, *24*, GB4018, doi:10.1029/2010GB003772.

Fritts, H. C. (1976), *Tree Rings and Climate*, Academic Press, New York.

Green, J. W. (1963), Wood cellulose, in *Methods in Carbohydrate Chemistry*, edited by R. L. Whistler, Academic Press, New York, pp. 9–21.

Grießinger, J., A. Bräuning, G. Helle, A. Thomas, and G. Schleser (2011), Late Holocene Asian summer monsoon variability reflected by $\delta^{18}O$ in tree-rings from Tibetan junipers, *Geophys. Res. Lett.*, *38*, L03701, doi:10.1029/2010GL045988.

Harris, I., P. D. Jones, T. J. Osborn, and D. H. Lister (2013), Updated high-resolution grids of monthly climatic observations – The CRU TS3.10 Dataset, *Int. J. Climatol.*, doi:10.1002/joc.3711.

Holmes, R. L. (1983), Computer-assisted quality control in tree-ring dating and measurement, *Tree-Ring Bull.*, *43*, 69–78.

Kagawa, A., and T. Nakatsuka (2013), *The Teflon-Container Method for Extracting Alpha-Cellulose Directly From Tree-Ring Laths, Paper Presented at Second American Dendrochronology Conference*, Tucson, Arizona.

Krishna Kumar, K., B. Rajagopalan, and M. A. Cane (1999), On the weakening relationship between the Indian monsoon and ENSO, *Science*, *284*, 2,156–2,159.

Krishnamurthy, V., and J. Shukla (2000), Intraseasonal and interannual variability of rainfall over India, *J. Clim.*, *13*, 4,366–4,377.

Krishnan, R., and M. Sugi (2003), Pacific decadal oscillation and variability of the Indian summer monsoon rainfall, *Clim. Dyn.*, *21*, 233–242.

Leavitt, S. W. (2010), Tree-ring C–H–O isotope variability and sampling, *Sci. Total Environ.*, *408*, 5,244–5,253.

Li, Q., T. Nakatsuka, K. Kawamura, Y. Liu, and H. Song (2011), Regional hydroclimate and precipitation $\delta^{18}O$ revealed in tree-ring cellulose $\delta^{18}O$ from different tree species in semi-arid Northern China, *Chem. Geol.*, *282*, 19–28.

Liu, X., W. An, K. Treydte, X. Shao, S. Leavitt, S. Hou, T. Chen, W. Sun, and D. Qin (2012), Tree-ring $\delta^{18}O$ in southwestern China linked to variations in regional cloud cover and tropical sea surface temperature, *Chem. Geol.*, *291*, 104–115.

Liu, X., X. Zeng, S. W. Leavitt, W. Wang, W. An, G. Xu, W. Sun, Y. Wang, D. Qin, and J. Ren (2013), A 400-year tree-ring $\delta^{18}O$ chronology for the southeastern Tibetan Plateau: Implications for inferring variations of the regional hydroclimate, *Global Planet. Change*, *104*, 23–33.

Loader, N. J., I. Robertson, A. C. Barker, V. R. Switsur, and J. S. Waterhouse (1997), An improved technique for the batch processing of small wholewood samples to α-cellulose, *Chem. Geol.*, *136*, 313–317.

Mantua, N. J., S. R. Hare, Y. Zhang, J. M. Wallace, and R. C. Francis (1997), A Pacific interdecadal climate oscillation with impacts on salmon production, *Bull. Am. Meteorol. Soc.*, *78*, 1,069–1,079.

May, W. (2002), Simulated changes of the Indian summer monsoon under enhanced greenhouse gas conditions in a global time-slice experiment, *Geophys. Res. Lett.*, *29*(7), 1118, doi:10.1029/2001GL013808.

McCarroll, D., and N. J. Loader (2004), Stable isotopes in tree rings, *Quat. Sci. Rev.*, *23*, 771–801.

Meehl, G. A., and W. M. Washington (1993), South Asian summer monsoon variability in a model with doubled atmospheric carbon dioxide concentration, *Science*, *260*, 1,101–1,104.

Naidu, C. V., K. Durgalakshmi, K. Muni Krishna, S. Ramalingeswara Rao, G. C. Satyanarayana, P. Lakshminarayana, and L. Malleswara Rao (2009), Is summer monsoon rainfall decreasing over India in the global warming era?, *J. Geophys. Res.*, *114*, D24108, doi:10.1029/2008JD011288.

Pant, G. B., and K. Rupa Kumar (1997), *Climates of South Asia*, John Wiley & Sons, Chichester.

Power, S., T. Casey, C. Folland, A. Colman, and V. Mehta (1999), Inter-decadal modulation of the impact of ENSO on Australia, *Clim. Dyn.*, *15*, 319–324.

Rayner, N. A., D. E. Parker, E. B. Horton, C. K. Folland, L. V. Alexander, D. P. Rowell, E. C. Kent, and A. Kaplan (2003), Global analyses of sea surface temperature, sea ice, and night marine air temperature since the late nineteenth century, *J. Geophys. Res.*, *108*(D14), 4407, doi:10.1029/2002JD002670.

Robertson, I., J. S. Waterhouse, A. C. Barker, A. H. C. Carter, and V. R. Switsur (2001), Oxygen isotope ratios of oak in east England: Implications for reconstructing the isotopic composition of precipitation, *Earth Planet. Sci. Lett.*, *191*, 21–31.

Roden, J. S., G. Lin, and J. R. Ehleringer (2000), A mechanistic model for interpretation of hydrogen and oxygen isotope ratios in tree-ring cellulose, *Geochim. Cosmochim. Acta*, *64*, 21–35.

Sano, M., F. Furuta, O. Kobayashi, and T. Sweda (2005), Temperature variations since the mid-18th century for western Nepal, as reconstructed from tree-ring width and density of *Abies spectabilis*, *Dendrochronologia*, *23*, 83–92.

Sano, M., M. S. Sheshshayee, S. Managave, R. Ramesh, R. Sukumar, and T. Sweda (2010), Climatic potential of $\delta^{18}O$ of *Abies spectabilis* from the Nepal Himalaya, *Dendrochronologia*, *28*, 93–98.

Sano, M., R. Ramesh, M. Sheshshayee, and R. Sukumar (2012a), Increasing aridity over the past 223 years in the Nepal Himalaya inferred from a tree-ring $\delta^{18}O$ chronology, *Holocene*, *22*, 809–817.

Sano, M., C. Xu, and T. Nakatsuka (2012b), A 300-year Vietnam hydroclimate and ENSO variability record reconstructed from tree ring $\delta^{18}O$, *J. Geophys. Res.*, *117*, D12115, doi:10.1029/12012JD017749.

Saurer, M., S. Borella, and M. Leuenberger (1997), $\delta^{18}O$ of tree rings of beech (*Fagus silvatica*) as a record of $\delta^{18}O$ of the growing season precipitation, *Tellus*, *49B*, 80–92.

Shi, C., et al. (2011), Sampling strategy and climatic implications of tree-ring stable isotopes on the southeast Tibetan Plateau, *Earth Planet. Sci. Lett.*, *301*, 307–316.

Shi, C., V. Daux, Q. B. Zhang, C. Risi, S. G. Hou, M. Stievenard, M. Pierre, Z. Li, and V. Masson-Delmotte (2012), Reconstruction of southeast Tibetan Plateau summer climate using tree ring $\delta^{18}O$: Moisture variability over the past two centuries, *Clim. Past*, *8*, 205–213.

Singh, J., and R. R. Yadav (2005), Spring precipitation variations over the western Himalaya, India, since A.D. 1731 as deduced from tree rings, *J. Geophys. Res.*, *110*, D01110, doi:10.1029/2004JD004855.

Stokes, M. A., and T. L. Smiley (1968), *An Introduction to Tree-Ring Dating*, University of Chicago Press, Chicago.

Szymczak, S., M. M. Joachimski, A. Bräuning, T. Hetzer, and J. Kuhlemann (2012), Are pooled tree ring $\delta^{13}C$ and $\delta^{18}O$ series reliable climate archives? — A case study of *Pinus nigra* spp. *laricio* (Corsica/France), *Chem. Geol.*, *308–309*, 40–49.

Tian, L., T. Yao, K. MacClune, J. W. C. White, A. Schilla, B. Vaughn, R. Vachon, and K. Ichiyanagi (2007), Stable isotopic variations in west China: A consideration of moisture sources, *J. Geophys. Res.*, *112*, D10112, doi:10.1029/2006JD007718.

Treydte, K. S., G. H. Schleser, G. Helle, D. C. Frank, M. Winiger, G. H. Haug, and J. Esper (2006), The twentieth century was the wettest period in northern Pakistan over the past millennium, *Nature*, *440*, 1,179–1,182.

Wang, B., and Q. Ding (2006), Changes in global precipitation over the past 56 years, *Geophys. Res. Lett.*, *33*, L06711, doi:10.1029/2005GL025347.

Webster, P. J., V. O. Magaña, T. N. Palmer, J. Shukla, R. A. Tomas, M. Yanai, and T. Yasunari (1998), Monsoons: Processes, predictability, and the prospects for prediction, *J. Geophys. Res.*, *103*, 14,451–14,510.

Wigley, T. M. L., K. R. Briffa, and P. D. Jones (1984), On the average value of correlated time series, with applications in dendroclimatology and hydrometeorology, *J. Clim. Appl. Meteorol.*, *23*, 201–213.

Wilson, R., A. Tudhope, P. Brohan, K. Briffa, T. Osborn, and S. Tett (2006), Two-hundred-fifty years of reconstructed and modeled tropical temperatures, *J. Geophys. Res.*, *111*, C10007, doi:10.1029/2005JC003188.

Wilson, R., E. Cook, R. D'Arrigo, N. Riedwyl, M. N. Evans, A. Tudhope, and R. Allan (2010), Reconstructing ENSO: The influence of method, proxy data, climate forcing and teleconnections, *J. Quat. Sci.*, *25*, 62–78.

Xu, C., M. Sano, and T. Nakatsuka (2011), Tree ring cellulose $\delta^{18}O$ of *Fokienia hodginsii* in northern Laos: A promising proxy to reconstruct ENSO?, *J. Geophys. Res.*, *116*, D24109, doi:10.1029/2011JD016694.

Xu, H., Y. Hong, and B. Hong (2012), Decreasing Asian summer monsoon intensity after 1860 AD in the global warming epoch, *Clim. Dyn.*, *39*, 2,079–2,088.

Yadav, R. R. (2011), Tree ring evidence of a 20th century precipitation surge in the monsoon shadow zone of the western Himalaya, India, *J. Geophys. Res.*, *116*, D02112, doi:10.1029/2010JD014647.

Yadav, R. R., W.-K. Park, and A. Bhattacharyya (1999), Spring-temperature variations in western Himalaya, India, as reconstructed from tree-rings: AD 1390–1987, *Holocene*, *9*, 85–90.

Yadav, R. R., W.-K. Park, J. Singh, and B. Dubey (2004), Do the western Himalayas defy global warming?, *Geophys. Res. Lett.*, *31*, L17201, doi:10.1029/2004GL020201.

Yasunari, T. (1979), Cloudiness fluctuations associated with the Northern Hemisphere summer monsoon, *J. Meteorol. Soc. Jpn.*, *57*, 227–242.

Yasunari, T. (1980), A quasi-stationary appearance of 30 to 40 day period in the cloudiness fluctuations during the summer monsoon over India, *J. Meteorol. Soc. Jpn.*, *58*, 225–229.

Yatagai, A., K. Kamiguchi, O. Arakawa, A. Hamada, N. Yasutomi, and A. Kitoh (2012), APHRODITE: Constructing a long-term daily gridded precipitation dataset for Asia based on a dense network of rain gauges, *Bull. Am. Meteorol. Soc.*, *93*, 1,401–1,415.

Young, G. H. F., J. C. Demmler, B. E. Gunnarson, A. J. Kirchhefer, N. J. Loader, and D. McCarroll (2011), Age trends in tree ring growth and isotopic archives: A case study of *Pinus sylvestris* L. from northwestern Norway, *Global Biogeochem. Cycles*, *25*, GB2020, doi:10.1029/2010GB003913.

Zhao, H., and G. W. K. Moore (2006), Reduction in Himalayan snow accumulation and weakening of the trade winds over the Pacific since the 1840s, *Geophys. Res. Lett.*, *33*, L17709, doi:10.1029/2006GL027339.

Zhou, T., R. Yu, H. Li, and B. Wang (2008a), Ocean forcing to changes in global monsoon precipitation over the recent half-century, *J. Clim.*, *21*, 3,833–3,852.

Zhou, T., L. Zhang, and H. Li (2008b), Changes in global land monsoon area and total rainfall accumulation over the last half century, *Geophys. Res. Lett.*, *35*, L16707, doi:10.1029/2008GL034881.